

The Potentially Hexadentate Isomeric Macrocycles *trans*- and *cis*-6,13-Diethyl-1,4,8,11-tetraazacyclotetradecane-6,13-diamine and Their Cobalt(III) Complexes: Unexpected Conformational Behavior

Paul V. Bernhardt,* Karl A. Byriel, Colin H. L. Kennard, and Philip C. Sharpe

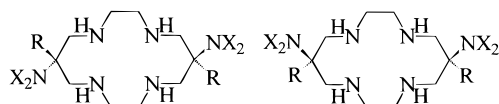
Department of Chemistry, University of Queensland, Brisbane 4072, Australia

Received September 28, 1995[⊗]

The new isomeric pendent arm macrocyclic hexaamines *trans*- and *cis*-6,13-diethyl-1,4,8,11-tetraazacyclotetradecane-6,13-diamine (L^5 and L^6) and their hexadentate coordinated cobalt(III) complexes are reported. X-ray crystal structural analyses of $[H_4L^5](ClO_4)_4 \cdot 2H_2O$ (triclinic, $P\bar{1}$, $a = 7.840(1)$ Å, $b = 13.6206(9)$ Å, $c = 14.246(1)$ Å, $\alpha = 77.141(6)^\circ$, $\beta = 86.539(9)^\circ$, $\gamma = 86.465(9)^\circ$, $Z = 2$) and $[CoL^5](ClO_4)_3$ (monoclinic, $C2/c$, $a = 14.461(6)$ Å, $b = 11.580(2)$ Å, $c = 15.865(5)$ Å, $\beta = 111.96(1)^\circ$, $Z = 4$) were performed. Cation disorder in the structure of $[CoL^5](ClO_4)_3$ is interpreted with the aid of molecular mechanics calculations, and solution conformational behavior is analyzed by NMR spectroscopy. It is found that the aqueous solution structure of $[H_4L^5]^{4+}$ is unusually ordered, by comparison with other closely related ligand systems.

Introduction

In previous reports, we have investigated the coordination chemistry of the isomeric hexaamines *trans*- and *cis*-6,13-dimethyl-1,4,8,11-tetraazacyclotetradecane-6,13-diamine (L^1 and L^2 , respectively).^{1,2} When coordinated as a hexadentate ligand, the *trans* isomer exhibits a coplanar array of the metal and four secondary amines with the pendent amines occupying *trans* sites, whereas the *cis* isomer adopts a folded configuration of the macrocycle with the pendent amines being *cis* disposed. It has been established clearly that hexadentate complexes of L^1 invariably exhibit unusually short M–N bond lengths and high energy d–d electronic transitions by comparison with other hexaamines, whereas hexadentate coordinated complexes of L^2 display properties that are not unusual when compared with those of hexaamine analogues.



L^1 R=Me, X=H	L^2 R=Me, X=H
L^3 R=Et, X=O	L^4 R=Et, X=O
L^5 R=Et, X=H	L^6 R=Et, X=H

Although complexes of each hexadentate bound ligand can exist in only one isomeric form, they may display conformational lability through the five-membered chelate rings defined by the macrocyclic portion of the complex. Molecular mechanics³ and angular overlap model⁴ calculations have established that the conformations of these chelate rings have a considerable bearing on the physical and structural properties of these complexes. Indeed, the preferred conformation of hexadentate coordinated complexes of L^1 is dependent on the metal ion size. In order to clarify the formerly ambiguous nomenclature

describing these conformers, we designate the relative (as opposed to absolute) configuration of the individual chelate ring conformations as *eq*, meaning that the H atom shown in Figure 1 is equatorial with respect to the five-membered chelate ring to which it is attached, or *ax*, when this same H atom is in an axial position. Small metal ions, such as Co(III),⁵ favor the eclipsed *trans*-*eq*,*eq* conformation whereas larger metal ions prefer the staggered *trans*-*eq*,*ax* (or enantiomeric *trans*-*ax*,*eq*) conformation. The third possibility, the eclipsed *trans*-*ax*,*ax* conformer, was predicted to be less stable for all but large metal ions ($M-N > 2.2$ Å). However, no metal ions larger than Zn(II), which exhibits the staggered *trans*-*eq*,*ax* conformation,⁶ have been able to be complexed by L^1 as a hexadentate.

In contrast, for hexadentate coordinated complexes of L^2 the *cis*-*ob*,*ob* conformation (Figure 1) was predicted to be dominant across the whole range of known M–N bond lengths. Also, the predicted M–N bond lengths were not unusual by comparison with other hexaamines. These predictions have been subsequently verified by the Cr(III),² Cd(II),⁷ and Pb(II)⁸ crystal structures of hexadentate coordinated L^2 complexes.

A report⁹ describing a number of nickel(II)-directed reactions leading to complexes of L^1 makes brief mention of the dinitro precursor of the diethyl-substituted analogue of L^1 (L^3). However, the possibility of *cis* or *trans* isomeric forms, *i.e.* L^3 and L^4 , was not addressed, nor was reduction to the respective hexaamines L^5 and L^6 attempted. To this end, we have investigated the coordination chemistry of both the *trans* and *cis* isomers of the diethyl analogues of L^1 and L^2 (L^5 and L^6 , respectively). Although, on face value, these systems might be expected to behave similarly, we have identified some unusual and significant structural and spectroscopic variations, simply upon substitution of “innocent” methyl groups by ethyl groups.

- Bernhardt, P. V.; Lawrance, G. A.; Hambley, T. W. *J. Chem. Soc., Dalton Trans.* **1989**, 1059.
- Bernhardt, P. V.; Lawrance, G. A.; Maeder, M.; Rossignoli, M.; Hambley, T. W. *J. Chem. Soc., Dalton Trans.* **1991**, 1167.
- Bernhardt, P. V.; Comba, P.; Hambley, T. W.; Lawrance, G. A.; Várnagy, K. *J. Chem. Soc., Dalton Trans.* **1992**, 355.
- Lye, P. G.; Lawrance, G. A.; Maeder, M.; Skelton, B. W.; Wen, H.; White, A. H. *J. Chem. Soc., Dalton Trans.* **1994**, 793.
- Curtis, N. F.; Gainsford, G. J.; Siriwardena, A.; Weatherburn, D. C. *Aust. J. Chem.*, **1993**, 46, 755.

[⊗] Abstract published in *Advance ACS Abstracts*, March 1, 1996.

- Bernhardt, P. V.; Comba, P.; Hambley, T. W.; Lawrance, G. A. *Inorg. Chem.* **1991**, 30, 942.
- Bernhardt, P. V.; Comba, P.; Hambley, T. W. *Inorg. Chem.* **1993**, 32, 2804.
- Bernhardt, P. V.; Comba, P. *Helv. Chim. Acta* **1991**, 74, 1834.
- Bernhardt, P. V.; Comba, P. *Inorg. Chem.* **1993**, 32, 2798.

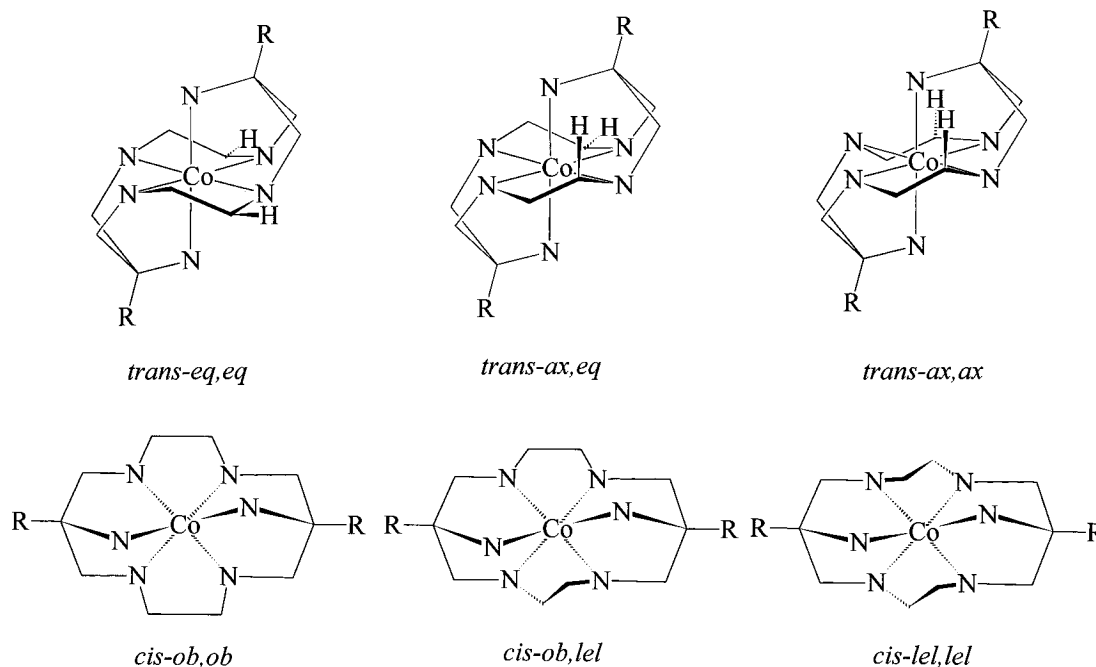


Figure 1. The nondegenerate conformations of $[ML^1]^{n+}$ ($R = \text{Me}$) and $[ML^5]^{n+}$ ($R = \text{Et}$) (above) and $[ML^2]^{n+}$ ($R = \text{Me}$) and $[ML^6]^{n+}$ ($R = \text{Et}$) (below). The H atoms shown define the axial or equatorial conformation of the five-membered chelate ring.

Experimental Section

Safety Note. Perchlorate salts are potentially explosive. Although we have experienced no problems with the compounds reported herein, they should only be handled in small quantities, and never scraped from sintered glass frits nor heated in the solid state.

Syntheses. All reagents were obtained commercially and were used without further purification. $\text{Na}_3[\text{Co}(\text{CO}_3)_3] \cdot 3\text{H}_2\text{O}$ was prepared from a literature synthesis.¹⁰

(trans/cis-6,13-Diethyl-6,13-dinitro-1,4,8,11-tetraazacyclotetradecane)copper(II) Perchlorate, $[\text{CuL}^3](\text{ClO}_4)_2/[\text{CuL}^4](\text{ClO}_4)_2$. To a stirred solution of $\text{Cu}(\text{NO}_3)_2 \cdot 3\text{H}_2\text{O}$ (25.0 g, 0.1 mol) in methanol (200 mL) was added slowly a mixture of ethylenediamine (13.5 mL, 0.20 mol) in methanol (25 mL). 1-Nitropropane (17 mL, 0.20 mol) and triethylamine (15 mL, 0.10 mol) were added to the resulting purple suspension, followed by aqueous formaldehyde solution (35 mL, 37%, 0.43 mol) in several portions. The reaction mixture was refluxed for 6 h, and then cooled in a refrigerator. The ensuing brown precipitate was collected by filtration, washed with ethanol three times, and air-dried. Recrystallization was achieved by suspending 24 g of crude product in water (50 mL), and then cautiously adding perchloric acid (10 mL, 70%) with stirring. The purple precipitate was collected by filtration, and the filtrate was discarded. The product was washed with ethanol and then diethyl ether and air-dried (18 g, 28%). Separation of this isomeric mixture of $[\text{CuL}^3](\text{ClO}_4)_2$ and $[\text{CuL}^4](\text{ClO}_4)_2$ was not attempted, but separation of the reduced amines was achieved as described below.

trans/cis-6,13-Diethyl-1,4,8,11-tetraazacyclotetradecane-6,13-diamine Hexahydrochloride, $[\text{H}_6\text{L}^5]\text{Cl}_6/[\text{H}_6\text{L}^6]\text{Cl}_6$. A solution of $[\text{CuL}^3](\text{ClO}_4)_2/[\text{CuL}^4](\text{ClO}_4)_2$ (16.7 g, 27 mmol) in hot water (1.5 L) was acidified with hydrochloric acid (150 mL, 32%). Excess granulated zinc (*ca.* 20 g) was added, and the suspension was stirred at 60 °C for 3 h, or until the solution became colorless. Gravity filtration was employed to remove solids, then the filtrate was charged onto a 400 × 60 cm column of Dowex 50W-X2 cation exchange resin (H^+ -form). The column was washed with 1 M HCl (*ca.* 2 L) until all traces of $\text{Zn}_{\text{aq}}^{2+}$ had eluted (tested by the appearance of $\text{Zn}(\text{OH})_2$ upon neutralization of aliquots of the eluate). The isomeric mixture of $[\text{H}_6\text{L}^5]^{6+}$ and $[\text{H}_6\text{L}^6]^{6+}$ was eluted with 5 M HCl (identified by addition of $\text{Cu}_{\text{aq}}^{2+}$ to a neutralized fraction of eluate to yield a purple, acid-stable solution) and was collected as a single fraction. A small amount of the eluate was evaporated to dryness, and the ^1H NMR spectrum of

this solid was consistent with a 3:1 ratio of $[\text{H}_6\text{L}^5]\text{Cl}_6$ and $[\text{H}_6\text{L}^6]\text{Cl}_6$ (see below). The major portion of the eluate was concentrated on a rotary evaporator to *ca.* 100 mL, and a colorless precipitate of $[\text{H}_6\text{L}^5]\text{Cl}_6$ was collected by filtration and washed with ethanol and then diethyl ether (4.0 g). The filtrate was evaporated to dryness to give an off-white mixture of $[\text{H}_6\text{L}^5]\text{Cl}_6$ and $[\text{H}_6\text{L}^6]\text{Cl}_6$ (4.1 g). The combined yield of both isomers was 56%.

Separation of $[\text{H}_6\text{L}^5]\text{Cl}_6$ and $[\text{H}_6\text{L}^6]\text{Cl}_6$. A sample of the above mixture of $[\text{H}_6\text{L}^5]\text{Cl}_6$ and $[\text{H}_6\text{L}^6]\text{Cl}_6$ (4.1 g) was dissolved in water (*ca.* 100 mL), a slight excess of $\text{Cu}(\text{NO}_3)_2 \cdot 3\text{H}_2\text{O}$ added, and then the pH of the solution was raised to ~5 with dilute NaOH solution. This solution was charged on a 1000 × 2 cm column of Dowex 50W-X2 cation exchange resin, and the column was washed with 1 M HCl to remove excess $\text{Cu}_{\text{aq}}^{2+}$. Five purple bands were observed with the following eluents (in parentheses): band 1 (1.4 M HCl, λ_{max} 529 nm); band 2 (1.7 M HCl, λ_{max} 542 nm); band 3 (1.7 M HCl, λ_{max} 536 nm); band 4 (3M HCl, λ_{max} 529 nm); band 5 (5 M HCl, λ_{max} 519 nm). Each band was separately reduced with zinc and rechromatographed on small Dowex columns (as above) to yield the ligands as their hexahydrochloride salts. Bands 1, 2, 3, and 5 were identified by ^1H NMR as $[\text{H}_6\text{L}^5]\text{Cl}_6$, and band 4 was $[\text{H}_6\text{L}^6]\text{Cl}_6$. Recovery of the ligands from the isomeric mixture was quantitative.

Anal. Calc for $[\text{H}_6\text{L}^5]\text{Cl}_6 \cdot 3\text{H}_2\text{O}$, $\text{C}_{14}\text{H}_{40}\text{Cl}_6\text{N}_6 \cdot 3\text{H}_2\text{O}$: C, 30.1; H, 8.3; N, 15.0. Found: C, 29.6; H, 8.2; N, 14.9. ^1H NMR (400 MHz, D_2O , pD ~ 2): δ 1.08 (t (triplet), CH_2CH_3 , 3J 7.6 Hz); 1.97 (q (quartet), CH_2CH_3); 3.09 and 3.23 (mult, $^2J(\text{AB}) - 13.0$, $^3J(\text{AA}') 11.8$, $^3J(\text{AB}') 1.7$, $^3J(\text{BB}') 4.0$ Hz, $\text{NCH}_2\text{CH}_2\text{N}$); 3.31 and 3.43 ppm (d (doublet), $^2J(\text{AB}) - 12.0$ Hz, NCH_2C). ^{13}C NMR (H-decoupled, D_2O , pD ~ 2): δ 6.5, 25.9, 47.6, 53.6, 56.2 ppm.

Anal. Calc for $[\text{H}_6\text{L}^6]\text{Cl}_6 \cdot 3\text{H}_2\text{O}$, $\text{C}_{14}\text{H}_{40}\text{Cl}_6\text{N}_6 \cdot 4\text{H}_2\text{O}$: C, 29.1; H, 8.4; N, 14.6. Found: C, 29.2; H, 8.0; N, 14.6. ^1H NMR (200 MHz, D_2O , pD ~ 2): δ 1.07 (t, CH_2CH_3 , 3J 7.6 Hz); 1.94 (q, CH_2CH_3); 3.18 (s (singlet), $\text{NCH}_2\text{CH}_2\text{N}$); 3.38 ppm (s, NCH_2C). ^{13}C NMR (H-decoupled, D_2O , pD ~ 2): δ 6.7, 26.4, 47.1, 53.2, 56.5 ppm.

trans-6,13-Diethyl-1,4,8,11-tetraazacyclotetradecane-6,13-diamine Tetrahydroperchlorate Dihydrate, $[\text{H}_4\text{L}^5](\text{ClO}_4)_4 \cdot 2\text{H}_2\text{O}$. To a solution of $[\text{H}_6\text{L}^5]\text{Cl}_6$ (0.30 g, 0.6 mmol) in water (6 mL) was added perchloric acid (0.5 mL, 70%). Upon standing at room temperature, the mixture deposited colorless prisms which were suitable for X-ray work. These were collected by filtration and air-dried (0.13 g, 30%). Further crops were obtained from the filtrate.

(trans-13-Ammonio-6,13-diethyl-1,4,8,11-tetraazacyclotetradecan-6-amine)aquacobalt(III) Perchlorate Hydrate, $[\text{Co}(\text{HL}^5)(\text{OH}_2)]-$

(10) Bauer, H. F.; Drinkard, W. C. *Inorg. Synth.* **1966**, *8*, 202.

(ClO_4)₄· H_2O . A solution of $[\text{H}_6\text{L}^5]\text{Cl}_6$ (2.62 g, 5.2 mmol) and $\text{Na}_3[\text{Co}(\text{CO}_3)_3]\cdot 3\text{H}_2\text{O}$ (1.93 g, 5.3 mmol) in water (200 mL) was heated at 90–95 °C for 2 h. The resulting solution was diluted to 2 L and charged onto a column of Sephadex C-25 cation exchange resin (Na^+ -form). Excess $\text{Co}_{\text{aq}}^{2+}$ was eluted with 0.2 M NaClO_4 solution. A second red band eluted with 0.4 M NaClO_4 solution. Upon concentration to ca. 50 mL, a red crystalline solid precipitated on standing and was collected by filtration, washed with ethanol, and air-dried (0.44 g, 10%). The microanalysis was consistent with cocrystallization of 1 equiv of sodium perchlorate per complex cation. Anal. Calc for $\text{C}_{14}\text{H}_{37}\text{Cl}_4\text{CoN}_6\text{O}_{17}\cdot\text{NaClO}_4\cdot\text{H}_2\text{O}$: C, 19.0; H, 4.2; N, 9.5. Found: C, 18.9; H, 4.5; N, 9.5. Electronic spectrum (H_2O): λ_{max} (ϵ , $\text{M}^{-1}\text{cm}^{-1}$) 519 nm (ϵ 66.8), 440 (ϵ 37.5), 357 (ϵ 91.3), 229 (ϵ 86 400). ^1H NMR (200 MHz, D_2O): δ 0.94 and 1.03 (t, CH_2CH_3 , 3J 7.7 Hz); 1.76 and 1.95 (q, CH_2CH_3); \sim 2.9, \sim 3.3, and \sim 3.7 (mult, CH_2) ppm. ^{13}C NMR (H-decoupled, D_2O): δ 6.6, 8.9, 27.9, 29.7, 52.0, 52.5, 54.0, 58.1, 60.4, 69.0 ppm.

(*trans*-6,13-Diethyl-1,4,8,11-tetraazacyclotetradecane-6,13-diamine)cobalt(III) Perchlorate Hydrate, $[\text{CoL}^5](\text{ClO}_4)_3\cdot\text{H}_2\text{O}$. In the above reaction, a third band eluted with 0.6 M NaClO_4 solution. The solution was concentrated to ca. 50 mL, and golden yellow crystals, suitable for X-ray work formed on standing. These were collected by filtration and washed with ethanol (0.72 g, 21%). Further crops were obtained from the filtrate. Anal. Calc for $\text{C}_{14}\text{H}_{34}\text{Cl}_3\text{CoN}_6\text{O}_{12}\cdot\text{H}_2\text{O}$: C, 25.4; H, 5.5; N, 12.7. Found: C, 25.2; H, 5.2; N, 12.6. Electronic spectrum (H_2O): λ_{max} (ϵ , $\text{M}^{-1}\text{cm}^{-1}$) 450 nm (ϵ 63.9), 330 (ϵ 64.1), 213 (ϵ 18 400). ^1H NMR (400 MHz, D_2O): δ 0.72 (t, CH_2CH_3 , 3J 7.7 Hz); 1.52 (q, CH_2CH_3); 2.61 and 3.25 (mult, $^2J(\text{AB})$ -14.9 , $^3J(\text{AA}')$ 8.0, $^3J(\text{AB}')$ 5.2, and $^3J(\text{BB}')$ 6.0 Hz, $\text{NCH}_2\text{CH}_2\text{N}$), 2.45 and 3.20 ppm (d, $^2J(\text{AB})$ -14.0 Hz, NCH_2C). ^{13}C NMR (H-decoupled, D_2O): δ 7.8, 26.9, 53.4, 58.3, 68.1 ppm.

(*cis*-6,13-Diethyl-1,4,8,11-tetraazacyclotetradecane-6,13-diamine)cobalt(III) Perchlorate Trihydrate, $[\text{CoL}^6](\text{ClO}_4)_3\cdot 3\text{H}_2\text{O}$. This compound was prepared in a manner identical to that for $[\text{CoL}^5](\text{ClO}_4)_3$ using $[\text{H}_6\text{L}^6]\text{Cl}_6$ as the ligand. Chromatographic purification (Sephadex C-25, 0.4 M NaClO_4) yielded a red pentadentate coordinated species, presumably $[\text{Co}(\text{L}^6)(\text{OH}_2)]^{3+}$, which eluted before the desired complex, but was not crystallized. The hexaamine $[\text{CoL}^6](\text{ClO}_4)_3$ precipitated upon concentration of the slow moving yellow band (yield 16% crystallized product). Anal. Calc for $\text{C}_{14}\text{H}_{34}\text{Cl}_3\text{CoN}_6\text{O}_{12}\cdot 3\text{H}_2\text{O}$: C, 24.1; H, 5.9; N, 12.0. Found: C, 23.8; H, 5.1; N, 11.9. Electronic spectrum (H_2O): λ_{max} (ϵ , $\text{M}^{-1}\text{cm}^{-1}$) 460 nm (ϵ 114), 336 (ϵ 88.4), 228 (ϵ 15 600). ^1H NMR (400 MHz, D_2O): δ 0.93 (t, CH_2CH_3 , 3J 7.7 Hz); 1.69 (q, CH_2CH_3); 2.67/3.52 and 3.26/2.87 (dd, NCH_2C , $^2J(\text{AB})$ -14.1 and -13.9 , $^4J(\text{AX})$ -1.9 Hz); 2.79 and 3.04 (td, $^2J(\text{AB}/\text{CD})$ -13.6 , $^3J(\text{AC})$ 13.5, and $^3J(\text{AD})$ 5 Hz, $\text{NCH}_2\text{CH}_2\text{N}$); 3.43 and 3.64 ppm (dd, $^3J(\text{BC})$ 4.4, $^3J(\text{BD})$ < 0.5 Hz). ^{13}C NMR (H-decoupled, D_2O): δ 7.5, 28.0, 54.2, 54.6, 58.1, 61.6, 71.5 ppm.

Physical Methods. Nuclear magnetic resonance spectra were measured at 200 (^1H) and 50.3 MHz (^{13}C) on a Bruker AC200 spectrometer. High-field 400 MHz ^1H NMR spectra were recorded on a JEOL GX400 instrument. Spectra were referenced with tetra-deuterated sodium 2,2-dimethyl-2-silapentane-5-sulfonate (DSS) (^1H) or with 1,4-dioxane (^{13}C), and all chemical shifts are cited *versus* tetramethylsilane. Simulations of NMR spectra were performed with the program DSYMPC.¹¹ Cyclic voltammetry was performed on a BAS 100B electrochemical analyzer employing a glassy carbon working electrode, a Pt auxiliary electrode, and a silver/silver chloride reference electrode. Potentiometric titrations were conducted on 1 mM solutions of the ligands in 0.5 M KNO_3 solution at 25 °C. Titrations were performed manually with a pH meter, and the data were analyzed with the program TITFIT.¹² Differential pulse polarography was performed on a Metrohm E506 instrument, employing a Metrohm E505 dropping mercury working electrode, a Pt auxiliary electrode, and a calomel reference electrode. All electrochemical solutions contained ca. 5 mM of complex in aqueous 0.1 M NaClO_4 and were purged with nitrogen before measurement. Electronic spectra were measured with a Beckman DU 7500 UV-vis spectrophotometer.

Table 1. Crystal Data

	$[\text{H}_6\text{L}^5](\text{ClO}_4)_4\cdot 2\text{H}_2\text{O}$	$[\text{CoL}^5](\text{ClO}_4)_3$
space group	$P\bar{1}$ (No. 2)	$C2/c$ (No. 15)
formula	$\text{C}_{14}\text{H}_{42}\text{Cl}_4\text{N}_6\text{O}_{18}$	$\text{C}_{14}\text{H}_{34}\text{Cl}_3\text{CoN}_6\text{O}_{12}$
a , Å	7.840(1)	14.461(6)
b , Å	13.6206(9)	11.580(2)
c , Å	14.246(1)	15.865(5)
α , deg	77.141(6)	
β , deg	86.539(9)	111.96(1)
γ , deg	86.465(9)	
V , Å ³	1478.6(2)	2464(1)
ρ_{calcd} , g cm ⁻³	1.627	1.735
fw	724.34	643.75
Z	2	4
μ , cm ⁻¹	4.87	10.9
temp, K	296	296
λ , Å	0.710 73	0.710 73
N	5194	2254
N_o ($F_o > 2\sigma$)	4624	1689
$2\theta_{\text{max}}$, deg	25	25
$R(F_o)$, ^a $wR_2(F_o^2)$ ^b	0.035, 0.093	0.059, 0.154

$$^a R(F_o) = \sum ||F_o| - |F_c|| / \sum |F_o|. \quad ^b wR_2(F_o^2) = (\sum w(F_o^2 - F_c^2)^2 / \sum wF_o^2)^{1/2}; w = 1/(\sigma^2(F_o^2) + (aP)^2 + bP); P = 1/3 \max(F_o^2, 0) + 2/3 F_c^2.$$

Molecular mechanics calculations were performed with the program MOMEPCP¹³ using a published force field.¹⁴

X-ray Crystal Structure Analyses. Intensity data for both compounds were measured on an Enraf-Nonius CAD4 four-circle diffractometer using graphite monochromated Mo $K\alpha$ radiation. Lattice dimensions were determined by a least-squares fit to the setting parameters of 25 independent reflections. The ω - 2θ scan technique was employed for both data sets. The intensities of three standard reflections were measured periodically (2 h), but no decay corrections were necessary. Data reduction and absorption correction were performed with the XTAL package.¹⁵ Both structures were solved by direct methods with SHELXS-86¹⁶ and refined by full-matrix least-squares analysis with SHELXL-93.¹⁷ All non-H atoms were refined with anisotropic thermal parameters, except for minor contributors to disorder. For the structure of $[\text{H}_6\text{L}^5](\text{ClO}_4)_4\cdot 2\text{H}_2\text{O}$, all H atoms were located and refined in (x , y , z , U_{iso}), whereas in $[\text{CoL}^5](\text{ClO}_4)_3$ all H atoms were restrained at estimated positions and their thermal parameters were fixed to 1.3 times that of the adjoining C or N atom. Crystallographic data are given in Table 1, and atomic coordinates appear in Tables 2 and 3. The atomic nomenclature is defined in Figures 2 and 4, drawn with the graphics program PLATON.¹⁸

Within the structure of $[\text{CoL}^5](\text{ClO}_4)_3$ there was found to be considerable disorder in the two independent perchlorate anions. The anion located at a general site exhibited two positions for each O atom, and these sites were refined with complementary occupancies. The perchlorate situated on a 2-fold axis was disordered about this site, and all four independent O atoms were constrained to have occupancies of 0.5. In addition, the five-membered chelate rings containing C(4) and C(5) exhibited disorder and the two sites for each C atom were also refined with complementary occupancies.

Results

The cyclization reaction leading to the isomeric mixture of $[\text{CuL}^3]^{2+}$ and $[\text{CuL}^4]^{2+}$ proceeded with similar efficiency to the synthesis of the dimethyl-substituted analogues.¹⁹ Similarly, an approximately 3:1 ratio of L^5 and L^6 was identified in the present

(11) Hägele, G.; Spiske, R.; Höffken, H. W.; Lenzen, T.; Weber, U.; Goudetsidis, S. *Phosphorus, Sulfur Silicon* **1993**, *77*, 262.
 (12) Zuberbühler, A. D.; Kaden, T. A. *Talanta* **1982**, *29*, 201.

(13) Comba, P.; Hambley, T. W. MOMEPCP: A Molecular Mechanics Program for Coordination Compounds. Universities of Heidelberg and Sydney, 1995.
 (14) Bernhardt, P. V.; Comba, P. *Inorg. Chem.* **1992**, *31*, 2638.
 (15) Hall, S. R.; Flack, H. D.; Stewart, J. M., Eds. The XTAL3.2 User's Manual. Universities of Western Australia, Geneva, and Maryland, 1992.
 (16) Sheldrick, G. M. *Acta Crystallogr.* **1990**, *A46*, 467.
 (17) Sheldrick, G. M. SHELXL93: Program for Crystal Structure Determination. University of Göttingen, 1993.
 (18) Spek, A. L. *Acta Crystallogr.* **1990**, *A46*, C34.

Table 2. Positional Parameters ($\times 10^4$) for $[\text{H}_4\text{L}^5](\text{ClO}_4)_4 \cdot 2\text{H}_2\text{O}$

	ligand 1 ($n = 1$)			ligand 2 ($n = 2$)		
	<i>x</i>	<i>y</i>	<i>z</i>	<i>x</i>	<i>y</i>	<i>z</i>
N(1 <i>n</i>)	-2006(2)	790(1)	-776(1)	-7075(2)	4144(1)	5549(1)
N(2 <i>n</i>)	-388(2)	1046(1)	834(1)	-4869(2)	4266(1)	3896(1)
N(3 <i>n</i>)	-2359(3)	3498(1)	-535(2)	-6844(3)	4638(2)	1750(1)
C(1 <i>n</i>)	-701(3)	2136(2)	470(2)	-5073(2)	3180(1)	4033(2)
C(2 <i>n</i>)	-2286(2)	2365(1)	-141(1)	-6845(2)	2883(1)	4499(1)
C(3 <i>n</i>)	-2079(3)	1914(1)	-1036(1)	-7103(3)	3060(1)	5526(2)
C(4 <i>n</i>)	-1616(3)	303(2)	-1608(2)	-7098(3)	4352(2)	6536(1)
C(5 <i>n</i>)	-1291(3)	-823(2)	-1266(2)	-6878(2)	5463(2)	6463(2)
C(6 <i>n</i>)	-3989(3)	2089(2)	418(2)	-8331(3)	3363(2)	3874(2)
C(7 <i>n</i>)	-4476(4)	2626(2)	1227(2)	-8227(4)	3238(2)	2842(2)
Cl(1)	3373(1)	1115(1)	8319(1)			
O(11)	4452(3)	1857(2)	7764(1)			
O(12)	4330(2)	512(2)	9091(2)			
O(13)	2839(3)	482(2)	7734(2)			
O(14)	1921(3)	1537(2)	8740(2)			
Cl(2)	-1880(1)	3553(1)	16422(1)			
O(21)	-821(2)	4215(1)	15722(1)			
O(22)	-2286(3)	3990(1)	17231(1)			
O(23)	-3429(2)	3462(2)	15974(1)			
O(24)	-1022(3)	2595(1)	16700(1)			
Cl(3)	-7597(1)	4426(1)	9181(1)			
O(31)	-7888(3)	5499(2)	8965(2)			
O(32)	-8857(3)	4026(2)	8704(2)			
O(33)	-5944(3)	4193(2)	8783(2)			
O(34)	-7749(4)	4047(2)	10184(2)			
Cl(4)	1162(1)	9101(1)	6153(1)			
O(41)	2362(3)	9818(2)	5708(2)			
O(42)	1815(3)	8516(2)	7023(2)			
O(43)	889(3)	8483(2)	5488(2)			
O(44)	-429(3)	9564(2)	6367(2)			
O(1)	-5682(3)	884(2)	3146(2)			
O(2)	3881(3)	8855(2)	4044(2)			

Table 3. Positional Parameters ($\times 10^4$) for $[\text{CoL}^5](\text{ClO}_4)_3$

	<i>x</i>	<i>y</i>	<i>z</i>
Co	2500	7500	0
N(1)	2034(3)	8873(3)	-752(2)
N(2)	1605(3)	7812(3)	636(3)
N(3)	3372(2)	8586(3)	883(2)
C(1)	1866(4)	8942(5)	1105(4)
C(2)	2655(3)	9532(4)	833(3)
C(3)	2262(5)	9901(4)	-158(3)
C(4) ^a	2363(6)	8819(6)	-1531(5)
C(5) ^a	3372(7)	8264(9)	-1203(6)
C(4') ^b	2927(17)	9063(18)	-1124(16)
C(5') ^b	3174(25)	7913(27)	-1407(21)
C(6)	3124(4)	10532(4)	1481(3)
C(7)	3946(6)	11183(6)	1319(5)
Cl(1)	871(1)	3019(1)	1198(1)
O(11) ^c	362(4)	3985(6)	634(4)
O(12) ^c	1910(3)	3105(5)	1426(5)
O(13) ^c	663(5)	3072(5)	2014(3)
O(14) ^c	493(5)	1963(5)	750(4)
O(11') ^d	1327(53)	3057(52)	2100(39)
O(12') ^d	1701(29)	2723(32)	875(29)
O(13') ^d	183(43)	3558(52)	425(39)
O(14') ^d	163(33)	2110(38)	1035(29)
Cl(2)	0	-605(2)	2500
O(21) ^e	-1011(11)	-1053(17)	2175(9)
O(22) ^e	634(16)	-1289(17)	2349(17)
O(23) ^e	198(9)	-604(20)	3484(8)
O(24) ^e	-62(15)	486(11)	2158(12)

^a Occupancy 0.79. ^b Occupancy 0.21. ^c Occupancy 0.92. ^d Occupancy 0.08. ^e Occupancy 0.5.

reaction, compared with a 4:1 ratio of L¹ and L².⁷ Separation of the isomeric reduced amines as their Cu(II) complexes, $[\text{Cu}(\text{H}_2\text{L}^5)]^{4+}$ and $[\text{Cu}(\text{H}_2\text{L}^6)]^{4+}$, was achieved by column chromatography on a strongly acidic cation exchange resin, a method initially employed for the separation of L¹ and L². Copper(II) complexes of these diamino-substituted 14-membered macro-

Table 4. Cation Bond Lengths (Å) for $[\text{H}_4\text{L}^5](\text{ClO}_4)_4 \cdot 2\text{H}_2\text{O}$ and $[\text{CoL}^5](\text{ClO}_4)_3$ ^a

	$[\text{H}_4\text{L}^5]^{4+}$ ($n = 1$)	$[\text{H}_4\text{L}^5]^{4+}$ ($n = 2$)	$[\text{CoL}^5]^{3+}$
Co-N(1)			1.951(4)
Co-N(2)			1.949(3)
Co-N(3)			1.953(3)
N(1 <i>n</i>)-C(3 <i>n</i>)	1.477(5)	1.489(5)	1.476(6)
N(1 <i>n</i>)-C(4 <i>n</i>)	1.493(5)	1.501(5)	1.483(7)
N(2 <i>n</i>)-C(5 <i>n</i>) ⁱ	1.469(5)	1.473(5)	1.531(9)
N(2 <i>n</i>)-C(1 <i>n</i>)	1.476(5)	1.466(5)	1.482(6)
N(3 <i>n</i>)-C(2 <i>n</i>)	1.513(5)	1.507(5)	1.490(5)
C(1 <i>n</i>)-C(2 <i>n</i>)	1.537(5)	1.535(5)	1.524(6)
C(2 <i>n</i>)-C(6 <i>n</i>)	1.532(5)	1.541(5)	1.528(6)
C(2 <i>n</i>)-C(3 <i>n</i>)	1.547(5)	1.543(6)	1.520(7)
C(4 <i>n</i>)-C(5 <i>n</i>)	1.531(5)	1.513(6)	1.498(11)
C(6 <i>n</i>)-C(7 <i>n</i>)	1.525(6)	1.522(7)	1.508(8)
N(1)-C(4')			1.62(2)
N(2)-C(5')			1.42(3)
C(4')-C(5')			1.49(4)

^a i denotes symmetry equivalent.

cyclic tetraamines⁷ and their macrobicyclic hexamine analogues²⁰ show remarkable resistance to acid-catalyzed dissociation by comparison with unsubstituted macrocyclic relatives. In addition, copper(II) complexes of 13-, 15-, or 16-membered macrocyclic analogues²¹ do not exhibit the same stability in strongly acidic solutions.

Recrystallization of $[\text{H}_6\text{L}^5]\text{Cl}_6$ from dilute aqueous HClO_4 afforded crystals of $[\text{H}_4\text{L}^5](\text{ClO}_4)_4 \cdot 2\text{H}_2\text{O}$. The X-ray crystal structural analysis of this compound revealed two independent macrocycles, each situated at centers of symmetry, with the anions and water molecules positioned at general sites. There are no significant differences between the corresponding bond lengths and angles of the two molecules (Tables 4 and 5), and their conformations are also the same. A view of one of the cations appears in Figure 2. An extensive array of H bonds is formed between amine H atoms and both anion and water O atoms. The sites of protonation were established by location and refinement of all amine H atoms from difference maps. The pendent primary amines on both macrocycles, N(3*n*), have been protonated as have pairs of centrosymmetrically-related secondary amines, N(1*n*), contained within each macrocyclic ring. Pairs of intramolecular H bonds are formed within each macrocyclic ring; N(1*n*)-H...N(2*n*) 2.04(3) Å ($n = 1$) and 2.13(3) Å ($n = 2$). By comparison, in the structures of $[\text{H}_4\text{L}^1](\text{ClO}_4)_4 \cdot 6\text{H}_2\text{O}$ ²² and $[\text{H}_4\text{L}^1]_3[\text{Fe}(\text{CN})_6]_4$,²³ similar conformations of the macrocyclic ring were identified. The dispositions of the pendent amines are the same in the structures of $[\text{H}_4\text{L}^1]_3[\text{Fe}(\text{CN})_6]_4 \cdot 6\text{H}_2\text{O}$ and $[\text{H}_4\text{L}^5](\text{ClO}_4)_4 \cdot 2\text{H}_2\text{O}$ (equatorial) but reversed in the structure of $[\text{H}_4\text{L}^1](\text{ClO}_4)_4 \cdot 6\text{H}_2\text{O}$, where the pendent amines adopt axial positions.

The protonation constants for L¹ and L² have been reported,^{6,8} with two $\text{p}K_a$ values around 11 and another two near 6 defining the first four protonation constants of the free base. Protonation of the remaining two amines is only achieved in concentrated acid. Preliminary potentiometric titrimetric data for L⁵·6HCl and L⁶·6HCl reveal a similar pairing of $\text{p}K_a$ values (L⁵ 5.1, 5.9,

(19) Comba, P.; Curtis, N. F.; Lawrance, G. A.; Sargeson, A. M.; Skelton, B. W.; White, A. H. *Inorg. Chem.* **1986**, *25*, 4260.

(20) Bernhardt, P. V.; Bramley, R.; Engelhardt, L. M.; Harrowfield, J. M.; Hockless, D. C. R.; Korybut-Daszkiwicz, B. R.; Krausz, E. R.; Morgan, T.; Sargeson, A. M.; Skelton, B. W.; White, A. H. *Inorg. Chem.* **1995**, *34*, 3589.

(21) Comba, P.; Curtis, N. F.; Lawrance, G. A.; O'Leary, M. A.; Skelton, B. W.; White, A. H. *J. Chem. Soc., Dalton Trans.* **1988**, 2145.

(22) Bernhardt, P. V.; Hambley, T. W.; Lawrance, G. A. *Aust. J. Chem.* **1990**, *43*, 699.

(23) Bernhardt, P. V.; Lawrance, G. A.; Skelton, B. W.; White, A. H. *Aust. J. Chem.* **1989**, *42*, 1035.

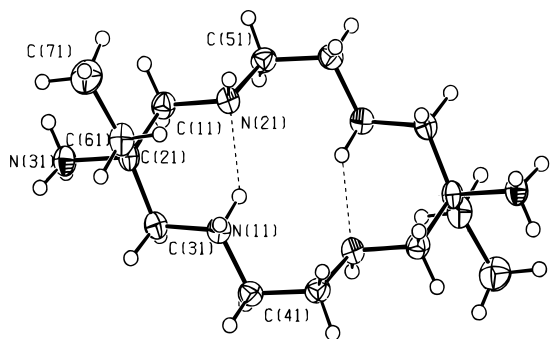


Figure 2. View of the cation $[\text{H}_4\text{L}^5]^{4+}$.

Table 5. Cation Bond Angles (deg) for $[\text{H}_4\text{L}^5](\text{ClO}_4)_4 \cdot 2\text{H}_2\text{O}$ and $[\text{CoL}^5](\text{ClO}_4)_3^a$

	$[\text{H}_4\text{L}^5]^{4+} (n = 1)$	$[\text{H}_4\text{L}^5]^{4+} (n = 2)$	$[\text{CoL}^5]^{3+}$
N(2)—Co—N(1)			91.2(2)
N(2)—Co—N(3)			83.4(2)
N(1)—Co—N(3)			84.1(2)
C(3)—N(1)—Co			108.8(3)
C(4)—N(1)—Co			109.3(3)
C(4')—N(1)—Co			101.1(7)
C(5') ⁱ —N(2)—Co			111.0(13)
C(1)—N(2)—Co			109.3(3)
C(5) ⁱ —N(2)—Co			106.3(4)
C(2)—N(3)—Co			100.7(2)
C(3n)—N(1n)—C(4n)	114.3(3)	114.3(3)	120.1(5)
C(3)—N(1)—C(4')			96.0(9)
C(1n)—N(2n)—C(5n) ⁱ	110.4(3)	111.7(3)	118.6(5)
C(1)—N(2)—C(5') ⁱ			99.0(13)
N(2n)—C(1n)—C(2n)	111.5(3)	111.4(3)	109.3(3)
N(3n)—C(2n)—C(3n)	104.3(3)	103.4(3)	104.2(3)
N(3n)—C(2n)—C(1n)	105.7(3)	105.7(3)	103.6(4)
C(3n)—C(2n)—C(1n)	111.9(3)	112.6(3)	112.9(4)
N(3n)—C(2n)—C(6n)	108.4(3)	109.5(3)	113.3(4)
C(3n)—C(2n)—C(6n)	110.5(3)	111.0(3)	112.6(4)
C(1n)—C(2n)—C(6n)	115.3(3)	113.9(3)	109.9(4)
N(1n)—C(3n)—C(2n)	111.4(3)	111.8(3)	110.0(4)
N(1n)—C(4n)—C(5n)	110.7(3)	109.6(3)	107.7(6)
C(4n)—C(5n)—N(2) ⁱ	109.7(3)	110.9(3)	111.0(6)
C(5')—C(4')—N(1)			108(2)
C(4')—C(5')—N(2) ⁱ			106(2)
C(7n)—C(6n)—C(2n)	115.3(4)	115.8(4)	116.4(4)

^a i denotes symmetry equivalent.

10.1, 11.0; L⁶ 4.9, 5.9, 9.7, 11.0). Again, the two remaining pK_a values for each system were too low to be determined potentiometrically. That is, the hexahydrochloride salts of the ligands L¹, L², L⁵, and L⁶ are hydrolyzed spontaneously to their tetraprotonated forms in aqueous solution. A more comprehensive study of the protonation and complexation equilibria involving L⁵ and L⁶ will be reported later.

The ¹H NMR spectrum of $[\text{D}_4\text{L}^5]^{4+}$ in D₂O exhibited a high degree of H—H coupling, with an AA'BB' pattern attributable to the protons of the ethylene diamine residues present (Figure 3). Additional resonances arise from the isolated methylene protons (AB) and the terminal ethyl group. The well-resolved AA'BB' coupling of protons attached to the macrocyclic ring of L⁵ is quite uncharacteristic of ligands such as these. By comparison, the ¹H NMR spectra of $[\text{D}_4\text{L}^1]^{4+}$ and $[\text{D}_4\text{L}^2]^{4+}$ in D₂O are relatively simple,⁷ with mere singlets arising from the ethylene protons and AB quartets from the isolated methylene protons. The fact that no H—H coupling within the ethylenediamine residues of L¹ or L² is observed indicates that this part of the macrocycle exhibits a number of conformations which interconvert rapidly on the NMR time scale. However, the observation of a second-order AA'BB' coupling pattern in the spectrum of $[\text{D}_4\text{L}^5]^{4+}$ indicates that one particular conformation is dominant relative to other possibilities. Indeed, the coupling

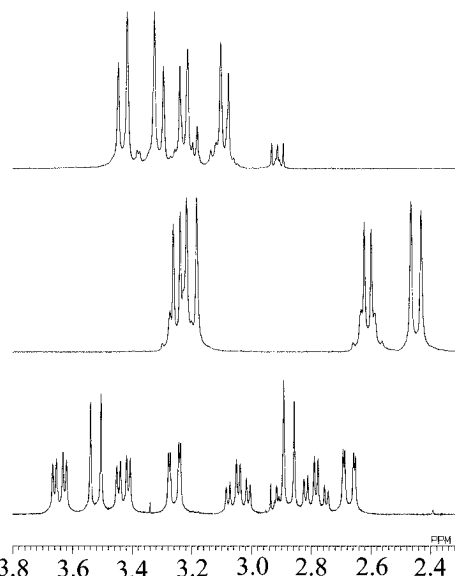


Figure 3. ¹H NMR spectra (400 MHz) of $[\text{D}_4\text{L}^5]^{4+}$ (top), $[\text{CoL}^5]^{3+}$ (center), and $[\text{CoL}^6]^{3+}$ (bottom) in D₂O (peaks at ca. 2.9 ppm due to DSS reference).

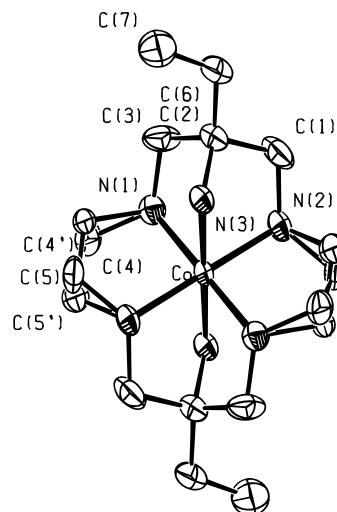


Figure 4. View of the disordered cation $[\text{CoL}^5]^{3+}$ (H atoms omitted for clarity).

constants obtained from simulation of the spectrum are consistent with a solid state conformation of $[\text{H}_4\text{L}^5]^{4+}$ being retained largely upon dissolution (see Discussion). By contrast, no coupling between any of the macrocyclic methylene protons is resolved in the ¹H NMR spectrum of $[\text{D}_4\text{L}^6]^{4+}$, and the solution structure of this ligand is clearly quite different from that of its isomeric relative.

Syntheses of the cobalt(III) complexes of L⁵ and L⁶ were achieved via methods analogous to those reported for their dimethyl analogues.^{2,5} The X-ray crystal structural analysis of $[\text{CoL}^5](\text{ClO}_4)_3$ found the complex cation to be situated on an inversion center, one perchlorate located on, and disordered about, a 2-fold axis, and another disordered perchlorate at a general site. Additional disorder in the macrocyclic five-membered chelate ring (N(1)—C(4)—C(5)—N(2a)) was identified, with the C atoms defining each puckered conformation being refined with complementary occupancies. A view of the disordered cation is presented in Figure 4. Analysis of this disorder will be deferred until the Discussion. The three independent Co—N bond lengths are not significantly different (Table 4) but are somewhat shorter than those typical of a (hexamine)cobalt(III) complex. However, the observed Co—N

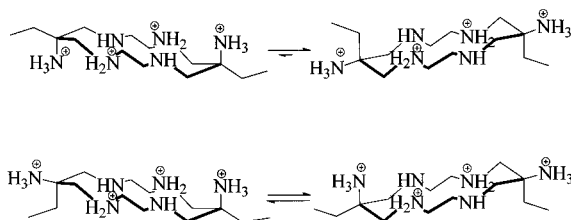


Figure 5. Equilibria between the axial and equatorial dispositions of the pendent ethyl groups of [H₄L⁵]⁴⁺ (above) and [H₄L⁶]⁴⁺ (below).

bond lengths are longer than those found in the structure of [CoL¹](ClO₄)Cl₂.⁵ The macrocyclic CoN₄ group is necessarily coplanar, and coordination of the pendent amines produces two fused five-membered chelate rings. The N–Co–N angles defined by these and all other five-membered chelate rings in the molecule are less than 90°, as anticipated (Table 5). The askew orientation of the ethyl group is similar to that found in the structure of [H₄L⁵]⁴⁺.

The ¹H NMR spectrum of [CoL⁵]³⁺ exhibited features similar to those found in the spectrum of [CoL¹]³⁺,² the most significant characteristics being the second-order AA'BB' coupling patterns, typical of a symmetrically 1,2-disubstituted ethyl group (Figure 3). An interpretation of the H–H coupling constants in relation to the solution structure of [CoL⁵]³⁺ will be deferred until the Discussion. The ¹H NMR spectrum of [CoL⁶]³⁺ (Figure 3) was very similar to that of its dimethyl analogue [CoL²]³⁺. A comprehensive analysis of the ¹H NMR spectrum of [CoL²]³⁺ has been given elsewhere,² and no further discussion is warranted here.

Cyclic voltammetry of the hexaamines [CoL⁵]³⁺ and [CoL⁶]³⁺ in aqueous solution yielded quasi-reversible ($\Delta E_p > 59$ mV) but chemically reversible Co^{III/II} couples ($i_a/i_c = 1.0$). The half-wave potentials, which were also determined polarographically, occurred at –0.58 and –0.48 V vs NHE for [CoL⁵]^{3+/2+} and [CoL⁶]^{3+/2+}, respectively. Notably, the [CoL⁵]^{3+/2+} couple occurred at a slightly more negative potential than that of the dimethyl analogue [CoL¹]^{3+/2+}² and is the most negative Co^{III/II} couple known for a hexaamine complex. This negative shift, which similarly occurs in going from [CoL²]^{3+/2+} to [CoL⁶]^{3+/2+}, is attributable to the greater electron-donating inductive effect of an ethyl group relative to a methyl group.

Discussion

The observation of a highly ordered solution structure of [H₄L⁵]⁴⁺ in contrast to all known analogues was unexpected and remarkable. The relatively strong intramolecular N–H···N bonds defined in the crystal structures of [H₄L⁵]⁴⁺ are not responsible for the observed rigid solution conformation. The same intramolecular H bond has been identified in the structures of [H₄L¹](ClO₄)₄·6H₂O,²¹ [H₄L¹]₃[Fe(CN)₆]₄·6H₂O,²² and [H₂L¹](ClO₄)₂·2H₂O,²⁴ but the solution structure of this ligand is fluxional.

In the absence of any other differences between [H₄L¹]⁴⁺ and [H₄L⁵]⁴⁺, it emerges that the pendent ethyl groups must play an active role in determining the overall solution structure of [H₄L⁵]⁴⁺, presumably by “locking” the overall conformation of the macrocycle, in a manner akin to that of bulky substituents attached to alicyclic hydrocarbons (Figure 5). When the pendent substituents are of a similar size, e.g. in [H₄L¹]⁴⁺ and [H₄L²]⁴⁺, the dispositions of these groups may interchange freely with a concomitant ruffling of the conformation of the 14-membered macrocyclic ring. The fact that [H₄L⁵]⁴⁺ appears to exhibit a

highly ordered and rigid solution structure implies that the ligand is preorganized for binding.

By comparison, the solution structure of [H₄L⁶]⁴⁺ exhibits no apparent order whatsoever but instead appears to be fluxional. If the macrocyclic ring conformation of [H₄L⁶]⁴⁺ is the same as that adopted by [H₄L⁵]⁴⁺, then one pendent ethyl group must be axial while the other is equatorial. Interchange of the dispositions of these groups results in no net change in energy, so the structure may fluctuate between these two degenerate conformers. The chemical shift differences between pairs of geminal protons are then averaged to zero. This argument is obviously similar to that proposed for the fluxional L¹ and L² systems in solution.

It should be mentioned that solid state conformations different from that identified for [H₄L⁵]⁴⁺ have been found in other protonated, 14-membered tetraazamacrocyclic ligands.²⁵ This raises the possibility that the solution conformation of [H₄L⁶]⁴⁺ is altogether different from that of [H₄L⁵]⁴⁺. Therefore, it will be of interest to examine whether the solid state structure of [H₄L⁶]⁴⁺ is markedly different from that of its respective *trans* isomer. These solution and solid state conformational aspects deserve further attention, and studies are currently underway in an effort to examine them in greater depth.

Disorder of the five-membered chelate rings identified in the crystal structure of [CoL⁵]³⁺ raises the question of the underlying geometry of the molecule represented in Figure 4. In a previous report,³ the conformational aspects of hexadentate coordinated complexes of L¹ and L² were investigated. It emerged that different conformations of [ML¹]ⁿ⁺ were favored for metal ions of various sizes. Briefly, the ordering of stability was found to be *trans*-*eq,eq* ~ *trans*-*eq,ax* (= *trans*-*ax,eq*) >> *trans*-*ax,ax* for small metal ions such as Co(III) and Fe(III). Looking at the observed crystal structure of [CoL⁵]³⁺, one can see that the refined model may be fitted to a number of combinations of the above four conformations. One possible solution would be a 72:28 mixture of the *trans*-*eq,eq* and *trans*-*ax,ax* conformers; the ratios being derived from the refined occupancies of C(4)/C(5) and C(4') and C(5'). Another solution would be a mixture of the *trans*-*eq,ax*, *trans*-*ax,eq* and *trans*-*eq,eq*, conformers in a 28:28:44 ratio; where the two enantiomeric conformers necessarily appear in the same proportion. It should be emphasized that there is no direct way in which these two models may be distinguished, as their averages both lead to the same observed geometry.

However, by the use of molecular mechanics, one can quantitatively examine the relative stabilities of these three nondegenerate conformers and thus make a more definitive assignment of the underlying geometry. It should be mentioned that the complexes [CoL⁵]³⁺ and [CoL⁶]³⁺ possess additional degrees of freedom from each of the three possible rotamers generated by torsion about the C(2)–C(6) bond, resulting in different dispositions of the pendent ethyl groups. Although these rotamers have no direct bearing on the conformation of each five-membered chelate ring, the relative energies of all the possible combinations have been considered when the complete conformational analysis was performed. The data are summarized in Table 6, in comparison with the observed and calculated Co–N bond lengths. It seems fairly clear from this analysis that the observed structure is a mixture of the *trans*-*ax,eq*, *trans*-*eq,ax*, and *trans*-*eq,eq* conformers in a 28:28:44 ratio. The three conformers obtained from this model of the experimental structure are shown in Figure 6. The minimized strain energies of the two nondegenerate conformers are similar

(24) Bernhardt, P. V.; Lawrance, G. A.; White, A. H. Unpublished results.

(25) Robinson, G. H.; Sangokoya, S. A.; Pennington, W. T.; Self, M. F.; Rogers, R. D. *J. Coord. Chem.* **1989**, *19*, 287.

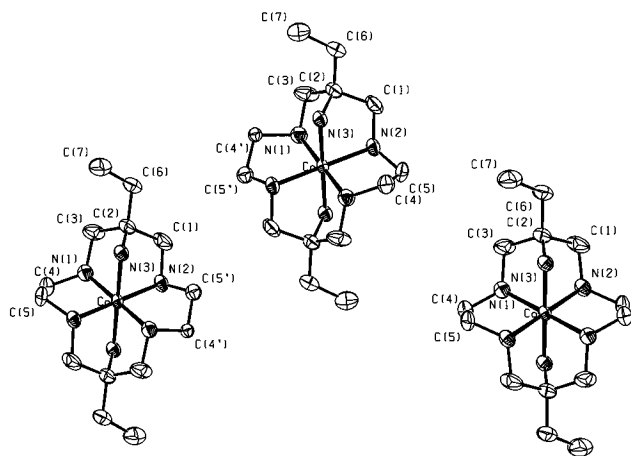


Figure 6. Views of the three contributors to the disordered structure of $[\text{CoL}^5]^{3+}$ (H-atoms omitted).

Table 6. Calculated (Molecular Mechanics) and Experimental (NMR) Conformer Proportions in Solution at 298 K

	conformer	Co–N _{av} , Å	calcd %	f_{eq}, f_{ob}	expt %
$[\text{CoL}^1]^{3+}$	<i>trans-eq,eq</i>	1.939	59	0.731	46
	<i>trans-eq,ax (ax,eq)</i>	1.951	41		54
	<i>trans-ax,ax</i>	1.969	0		0
$[\text{CoL}^5]^{3+}$	<i>trans-eq,eq</i>	1.938	53	0.666	33
	<i>trans-eq,ax (ax,eq)</i>	1.949	47		67
	<i>trans-ax,ax</i>	1.967	0		0
$[\text{CoL}^2]^{3+}$	<i>cis-ob,ob</i>	1.951	88	1.0	100
	<i>cis-ob,lcl (lcl,ob)</i>	1.951	12		0
	<i>cis-lcl,lcl</i>	1.946	0		0
$[\text{CoL}^6]^{3+}$	<i>cis-ob,ob</i>	1.950	88	1.0	100
	<i>cis-ob,lcl (lcl,ob)</i>	1.950	12		0
	<i>cis-lcl,lcl</i>	1.945	0		0
$[\text{H}_4\text{L}^5]^{4+}$	<i>trans-eq,eq</i>			0	0
	<i>trans-eq,ax (ax,eq)</i>				0
	<i>trans-ax,ax</i>				100

and both significantly smaller than that of the *trans-ax,ax* conformer. The observed Co–N bond lengths are also consistent with an averaging of *trans-ax,eq/trans-eq,ax* (Co–N ~ 1.95 Å) and *trans-eq,eq* (Co–N ~ 1.94 Å) conformers.

The solution conformational structure of $[\text{CoL}^5]^{3+}$ was investigated by ^1H NMR. Analysis of the vicinal H–H coupling constants within five-membered chelate rings may lead to an overall picture of the conformer distribution in solution. The observed vicinal coupling constants (Experimental Section) will be weighted averages of the actual coupling constants in the two possible conformations, *eq* and *ax*. The appropriate equations relating these coupling constants to the ratio of each conformation have been described previously,²⁶ and no further elaboration will be given here. The results of this analysis appear in Table 6.

It emerges that the complexes $[\text{CoL}^1]^{3+}$ and $[\text{CoL}^5]^{3+}$ exist in solution as mixtures of the *trans-eq,eq* and *trans-ax,eq/trans-eq,ax* conformers. In both cases, the relative proportions of these conformers in solution are significantly different from those found in their solid state structures. Compared with an approximately 3:2 ratio of *trans-eq,eq:(trans-ax,eq + trans-eq,ax)* found in solution, the crystal structural analysis of $[\text{CoL}^1]-(\text{ClO}_4)_2$ found the cation exclusively in the *trans-eq,eq* conformation, with no disorder of the five-membered chelate rings being found. Significantly, the isostructural $[\text{FeL}^1](\text{ClO}_4)_2$ does exhibit disorder of the five-membered chelate rings,¹ as does the same complex cation crystallized in a different

lattice.²⁷ That is, disorder in the $[\text{FeL}^1]^{3+}$ cation is independent of the lattice, and the observed differences between the structures of $[\text{CoL}^1](\text{ClO}_4)_2$ and $[\text{FeL}^1](\text{ClO}_4)_2$ reflect variations in the relative stabilities of the two relevant conformations with changes in metal ion size. This is consistent with molecular mechanics predictions⁵ that the *trans-ax,eq/trans-eq,ax* conformers become increasingly favored relative to the *trans-eq,eq* conformer with increasing metal ion size. In the crystal structure of $[\text{CoL}^5](\text{ClO}_4)_3$, the *trans-eq,eq:(trans-ax,eq + trans-eq,ax)* ratio was found to be approximately 1:1, in contrast to the 1:4 ratio found in solution.

The NMR data indicate that the *cis-ob,ob* conformers of $[\text{CoL}^1]^{3+}$ and $[\text{CoL}^6]^{3+}$ are dominant in solution ($f_{ob} \sim 1$). Molecular mechanics calculations have predicted that this conformer will always be favored no matter how large or small the M–N bond length becomes, and all existing solid state and solution data for these systems are consistent with this.

The ^1H NMR data relating to $[\text{H}_4\text{L}^5]^{4+}$ indicate that the $\text{NCH}_2\text{-CH}_2\text{N}$ group exists in one major conformation. The same rigorous conformational analysis that has been applied to $[\text{CoL}^5]^{3+}$ and $[\text{CoL}^6]^{3+}$ cannot be applied strictly to the metal-free ligand, as it possesses greater conformational freedom. However, if we make the assumptions that the ligand may adopt either of the two conformations shown in Figure 5 and that the H–C–C–H dihedral angles interconvert upon going from one conformer to the other, *i.e.* $\phi_{eqAA'} = \phi_{axBB'}$, $\phi_{eqBB'} = \phi_{axAA'}$ and $\phi_{eqAB'} = \phi_{axAB'}$, then a similar analysis may be performed. These dihedral angles were similar to those found in the crystal structure of $[\text{H}_4\text{L}^5](\text{ClO}_4)_4$. The results of this analysis (Table 6) indicate that only one conformation of $[\text{H}_4\text{L}^5]^{4+}$ is present to any significant degree in solution, and this is presumably the same conformation identified in the crystal structure analysis, which may be described as *trans-ax,ax* in keeping with the nomenclature defined in Figure 1.

It is informative to examine the possible routes by which conformational interconversion occurs within the $[\text{CoL}^1]^{3+}$ and $[\text{CoL}^2]^{3+}$ systems. Disregarding the rotational lability of the pendent ethyl groups on $[\text{CoL}^5]^{3+}$ and $[\text{CoL}^6]^{3+}$, the same arguments are applicable to the diethyl-substituted analogues. It is clear that each of these complexes possess only two conformational degrees of freedom, *i.e.* those being the N–C–C–N dihedral angles defined by their macrocyclic five-membered chelate rings. That is, interconversion of the four possible (three nondegenerate) conformers of each isomer occurs along these coordinates. Therefore, with molecular mechanics,²⁸ one can map the entire conformational space of each isomer as a function of these two dihedral angles, and the results appear in Figures 7 and 8. Looking at the surface for $[\text{CoL}^1]^{3+}$, we see the anticipated minima corresponding to the four possible combinations of the *ax* and *eq* conformations of the two five-membered chelate rings. The surface necessarily has C_s symmetry, illustrating the enantiomeric relationship between structures on either side of the mirror plane of the surface. As expected, saddle points occur on the surface when either N–C–C–N dihedral angle passes through 0° . One of the most important points to emerge from this plot is the route by which the conformers should interconvert. The pathways of minimum energy involve the inversion of only one chelate ring at a time, *i.e.* *trans-eq,eq* \rightarrow *trans-eq,ax* \rightarrow *trans-ax,ax* \rightarrow *trans-ax,eq* \rightarrow *trans-eq,eq*. The calculations indicate that inversion of both chelate rings simultaneously, *i.e.* *trans-eq,eq* \rightarrow *trans-ax,ax* or *trans-ax,eq* \rightarrow *trans-eq,ax*, is highly unlikely on the basis of

(27) Bernhardt, P. V.; Hambley, T. W.; Lawrance, G. A. *J. Chem. Soc., Chem. Commun.* **1989**, 553.

(28) Hambley, T. W. *J. Comput. Chem.* **1987**, 8, 651.

(26) Sudmeier, J. L.; Blackmer, G. L. *Inorg. Chem.* **1971**, 10, 2010.

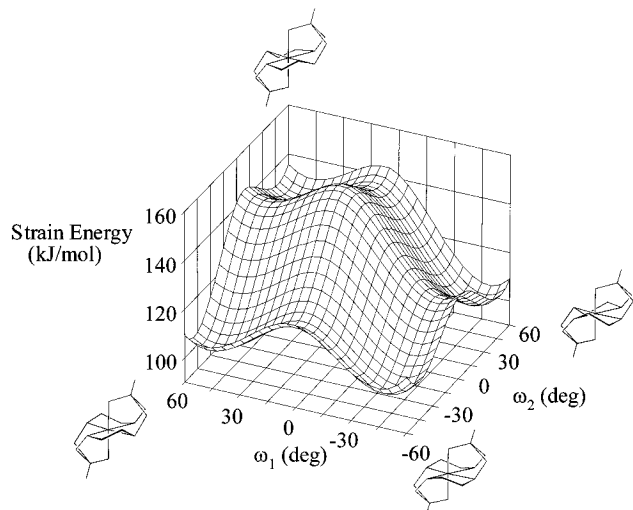


Figure 7. Molecular mechanics conformational potential energy surface for $[\text{CoL}^1]^{3+}$ as a function of the two N–C–C–N dihedral angles, ω_1 and ω_2 (deg).

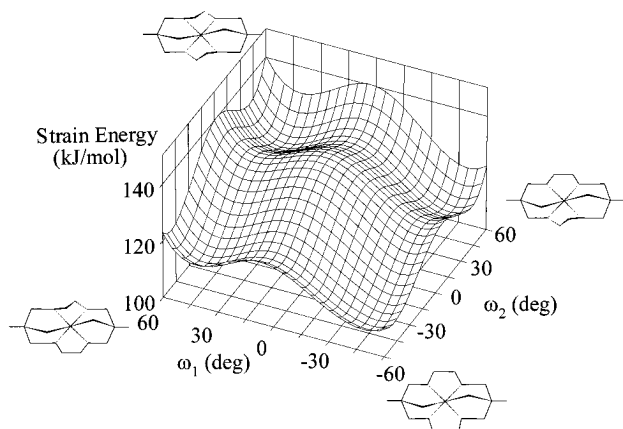


Figure 8. Molecular mechanics conformational potential energy surface for $[\text{CoL}^2]^{3+}$ as a function of the two N–C–C–N dihedral angles, ω_1 and ω_2 (deg).

strain energy, with a much greater activation barrier being predicted. Statistical factors would also disfavor this route. The relative populations of these wells (Table 6) are determined by the respective strain energies in each minimum, but the activation barriers between the minima ($\sim 20 \text{ kJ mol}^{-1}$) are sufficiently low that the conformers interconvert rapidly on the NMR time scale, on the basis of experimentally determined vibrational frequencies for closely related chelate ring systems.²⁹

The surface corresponding to $[\text{CoL}^2]^{3+}$ (Figure 8) exhibits features similar to those of that corresponding to $[\text{CoL}^1]^{3+}$. In this case, the lowest energy minimum (*cis-ob,ob*) is sufficiently more stable than the others such that it is populated almost exclusively at room temperature. The activation barriers are

similar to those found in $[\text{CoL}^1]^{3+}$, and the pathways between each conformer also involve the inversion of a single chelate ring at a time.

The crucial factor that favors one conformation of $[\text{ML}^1]^{n+}$ over another is the M–N bond length. However, when variations between closely related systems such as $[\text{CoL}^1]^{3+}$ and $[\text{CoL}^5]^{3+}$ are compared, the factors that influence these differences in solution conformational behavior are less clear. Although molecular mechanics calculations qualitatively predict that the *trans-eq,ax:trans-eq,eq* conformational ratio increases for $[\text{CoL}^5]^{3+}$ relative to $[\text{CoL}^1]^{3+}$, the observed 1:4 *trans-eq,eq:(trans-eq,ax + trans-ax,eq)* ratio was not predicted by the calculations. Factors other than steric strain, such as solvation and ion pairing, are probably of equal importance in these systems. In this case, the pendent ethyl groups of $[\text{CoL}^5]^{3+}$ increase the hydrophobicity of the molecule in addition to their internal steric influence. Further work needs to be done to delineate these competing effects, and further speculation is not warranted, at present.

It has been established that the conformation of chelate rings within $[\text{CoL}^1]^{3+}$ and $[\text{CoL}^2]^{3+}$, and other related hexaamines, has a significant bearing on their Co–N bond lengths. Consequently, the ligand field spectra of these molecules will be sensitive to the conformation of the molecule. Therefore, if one can understand more completely the factors that trigger a conformational change from one form to another, then the possibility arises for conformationally switched chromophores. The inherent complexities and ambiguities in both the interpretation of solution structures and in the relative insensitivity of many of these chromophores to conformational change have resulted in there being few examples where an unequivocal solution structure of a conformationally labile system such as this has been obtained. In a recent report,³⁰ it emerged that significant conformational disparities can occur between complexes exhibiting very similar ligand systems and that these variations cannot be attributed solely to steric strain. Further investigations of intermolecular effects such as solvation and ion pairing need to be considered in tandem with intramolecular steric effects in order to obtain a clearer picture of what is a complex problem.

Acknowledgment. We thank Lynette Lambert for measuring the high-field NMR spectra, and financial support from a Departmental Startup Grant to P.V.B. is gratefully acknowledged.

Supporting Information Available: Tables giving full crystal and refinement data, thermal parameters, H atom positional parameters, and bond lengths and angles (13 pages). Ordering information is given on any current masthead page.

IC951260Y

(29) Niketic, S. R.; Rasmussen, K. *Acta Chem. Scand.* **1981**, A35, 213.

(30) Bernhardt, P. V.; Bygott, A. M. T.; Geue, R. J.; Hendry, A. J.; Korybut-Daszkiewicz, B. R.; Lay, P. A.; Pladzewicz, J. R.; Sargeson, A. M.; Willis, A. C. *Inorg. Chem.* **1994**, 33, 4553.